Modelling the effect of phase transition on the blast wave in BLEVEs

Knut Vaagsaether, Osama Kabbashi Mohammed Ibrahim, Per Morten Hansen, Dag Bjerketvedt
University of South-Eastern Norway
Porsgrunn, Norway

1 Introduction

The main interest in this work is the rapid expansion of fluid due to phase transition that will contribute to a blast wave in a BLEVE scenario. The study uses saturated liquid CO2 as medium. The use of carbon dioxide as a medium is a practical one since it is relatively safer to use in experiments than other liquefied gasses like propane or ammonia. The downside of using CO2 is that the fluid will cross the triple point during depressurization, leading to solid/gas two phase flow at lower pressures. However, in the present work this process is assumed slow and is not included since it is doubtful that it will impact on the blast wave caused by the initial fast phase transition. Figure 1 shows the isentropic expansion path of liquid CO2 into the metastable region. The kinetic spinodal are limits for expansion where a significant generation rate of critical bubbles is reached. The kinetic spinodal for heterogeneous nucleation assumes that the critical work to generate bubbles in the liquid is half the critical work for the bulk. The thermodynamic states are calculated by using an equation of state (EOS) based on Helmholtz free energy [1] and [2].

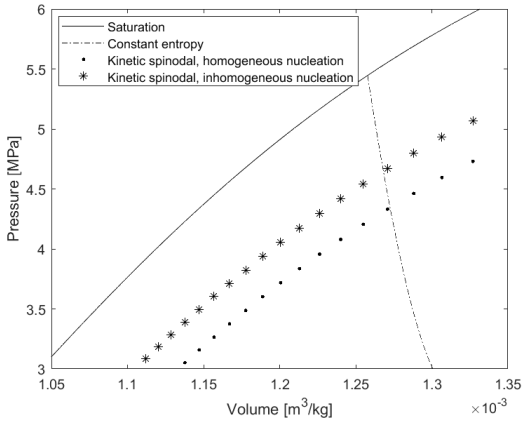

Figure 1: Pressure-volume diagram for CO2 showing an isentrope from saturated liquid at 291 K and the kinetic spinodals for homogeneous and inhomogeneous nucleation.

Correspondence to: knutv@usn.no

2 Method

The present simulation method is based on Classical Nucleation Theory [3] and uses the production rate of critical bubbles as a source in a two-fluid multiphase equation set. The most important equations from the Classical Nucleation Theory are included here for completeness.

The rate of creation of a number of critical size bubbles pr. volume is calculated as equation 1.

$$dJ = J_0 \exp\left(-\frac{W_{cr}}{kT_0}\right), \tag{1}$$

The critical work is here simplified to eq. 2 by assuming the Poynting factor to be unity.

$$W_{cr} = \frac{16\pi\sigma^3}{3\left(p_{sat}(T)-p(T)\right)^2}, \tag{2}$$

Where J_0 – initial possible nucleation sites, k – Boltzmann constant, T_0 – critical temperature, σ – liquid/gas surface tension.

The critical work needed during the inhomogeneous nucleation at the wall is assumed to be half of the critical work in the bulk. This reduction in critical work will be dependent on surface roughness and the values of 0.5 is assuming a 90° contact angle between droplet and wall.

2.1 Computational Fluid Dynamics

A two-fluid model for CFD simulations of the process uses mass, momentum, and energy conservation of two immiscible fluids (liquid and gas phases) [4]. One assumption in using this model is that the momentum of each phase is given by a common velocity, leading to a six-equation model in 2D. Equations 3 and 4 are equations for mass conservation of the two phases, equation 5 is the equation for the common momentum, equations 6 and 7 are the energy equations for each phase.

$$\frac{\partial \rho_1 \alpha_1}{\partial t} + \nabla \cdot (\rho_1 \alpha_1 \vec{u}) = -\dot{R}, \tag{3}$$

$$\frac{\partial \rho_2 \alpha_2}{\partial t} + \nabla \cdot (\rho_2 \alpha_2 \vec{u}) = \dot{R}, \tag{4}$$

$$\frac{\partial \rho u_i}{\partial t} + \nabla \cdot (\rho \vec{u} u_i) + \frac{\partial p}{\partial x_i} = 0, \tag{5}$$

$$\frac{\partial \alpha_1 E_1}{\partial t} + \nabla \cdot (\alpha_1 \vec{u}(E_1 + p)) = -\dot{R} Q_{\text{vap}}, \tag{6}$$

$$\frac{\partial \alpha_2 E_2}{\partial t} + \nabla \cdot \left(\alpha_2 \vec{u}(E_2 + p)\right) = \dot{R} Q_{vap}, \tag{7}$$

Where α_1 is the volume fraction of liquid and α_2 is the volume fraction of the gas. The volume fractions are related as $\alpha_1 + \alpha_2 = 1$ and $\rho_1\alpha_1 + \rho_2\alpha_2 = \rho$. The energies of each phase are calculated as equation 8.

And, p – pressure, u – fluid velocity, ρ – fluid density, Q_{vap} – heat of evaporation.

$$E_i = e_i + \frac{1}{2}\rho_i |\vec{u}|^2, \tag{8}$$

For the liquid phase, a stiffened gas equation of state is used to model the dependence of internal energy to pressure (see equation 9).

$$e_1 = \frac{p+\gamma_1 p_\infty}{\gamma_1 - 1}, \tag{9}$$

Ideal gas law is used for the gas phase (phase 2), equation 10.

$$e_2 = \frac{p}{\gamma_2 - 1} + e^*, \tag{10}$$

The constant e* is an energy term to set the correct difference in internal energy between the gas and liquid phase. Since the modelled internal energy is based on changes in internal energy, this term must be added to model the correct change of energy between the phases. The Flux Limiter Centered Scheme (FLIC) is used to solve the equations' hyperbolic parts, while a Newton-Rhapson iterative solver is needed to isolate volume fraction and pressure from the conserved mass and energies.

The phase transition mass rate, $\dot{R}$ in equation 11, is modeled using the nucleation rate in eq. 1.

$$\dot{R} = \rho_{g,sat}(T) V_{cr} dJ, \tag{11}$$

Where V_{cr} is the volume of a critical bubble and ρ_{sat} is the gas density of the critical bubbles. The radius of a critical bubble is calculated as equation 12.

$$r_{cr} = \frac{2\sigma}{p_{sat}(T) - p}, \tag{12}$$

The mass and energy sources are solved using Godunov splitting so that the hyperbolic part is solved using the FLIC scheme, and the sources are solved by a simple first-order Euler method. Table 1 shows the model constants used in the present work. The constants are obtained by fitting the internal energy and sound speed from the model to values from the Helmholtz free energy-based EOS along a constant entropy process from saturated liquid at 291 K into the metastable region. The choice of the fitting region is small but relevant for the expansion process of the liquid before the onset of nucleation.

Table 1: Model constants for CO2

Variable	Value
γ_1	1.066
γ_2	1.32
p_∞	$7.3 \cdot 10^7$ Pa
e*	$1.62 \cdot 10^6$ J/kg
σ	$2.0 \cdot 10^{-3}$ N/m
Q_{vap}	$1.8 \cdot 10^5$ J/kg

The experiments used as validation data have been published [5], but a short description is provided here. Figure 2 shows the experimental set-up where saturated liquid CO2, with a saturated vapor head, is filled into a conical vessel. A double membrane release system is placed on top of the conical vessel. The double membrane system separates the high pressure, conical vessel, from the surroundings by two membranes, where the volume between the membranes will have a medium pressure of CO2 before rupture. The rupture procedure is done by increasing the pressure in the separating volume up until the top membrane ruptures. The subsequent pressure-drop leads to rupture of the lower membrane initiating the depressurization of the CO2 in the conical vessel. The conical vessel has an angle of 4^o to the center axis and is ID 90 mm at the top. A polycarbonate pipe of ID 90 mm is fitted above the membrane system to be able to measure the blast wave from the depressurization of the fluid.

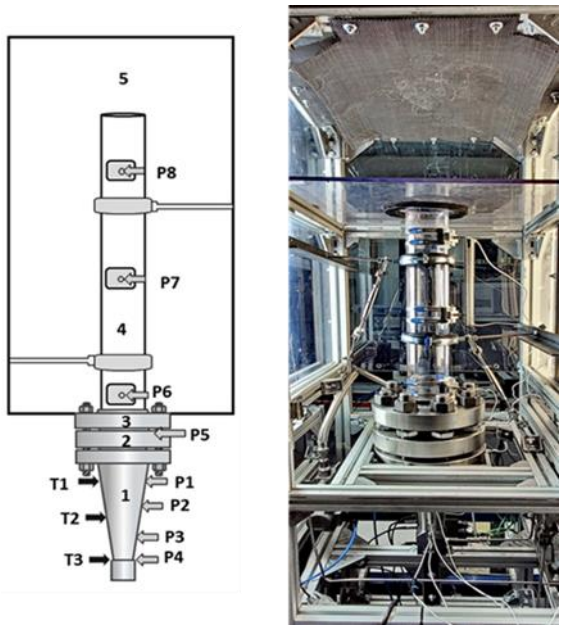

Figure 2: Schematic drawing of the setup on the left-hand side: 1- HP conical vessel, 2- MP slip-on flange, 3- upper flange opened to atmospheric pressure, 4- polycarbonate tube, 5- chamber. An image of the installation is on the right-hand side.

3 Results and discussion

The simulations were done in 2D axis symmetry, where the center axis of the geometry follows the conical vessel's center axis. The simulation also includes the rupture of the top diaphragm before the depressurization of the conical vessel is initiated. The timing of the rupture of the bottom diaphragm will be off in the simulation compared to the experiments since the response time of the material will not be simulated. The rupture of the top diaphragm and subsequent blast from the compressed CO2 in the medium pressure volume will be seen as a shock wave propagating through the polycarbonate pipe. Figure 3 shows the pressure history of pressure sensor P2 located 185 mm from the “bottom” of the conical vessel for 35 and 73 % liquid volume fraction. The sensor is initially in the liquid phase. The first pressure drop after about 3 ms is the first rarefaction wave due to the sudden opening of the diaphragm. The state behind the rarefaction wave will be metastable liquid as the pressure is held at the kinetic spinodal pressure due to pressure increase of the phase transition. A phase transition front is following the rarefaction wave as is seen as a sudden pressure drop at about 5-6 ms. The timing of the simulated phase transition front compared to the experimental results is somewhat delayed. The simulations will behave very ideally compared to an experiment as no stresses in the fluid, except from pressure, are simulated. The assumption of lower critical work at the wall by a factor of two is also not justified here. This factor may be significantly higher due to wall surface roughness and further work is needed to determine this effect. The linear equations of state used in the simulations will lead to erroneous speeds of sound and fluid expansion in the metastable region as the compressibility will be handled as an ideal gas.

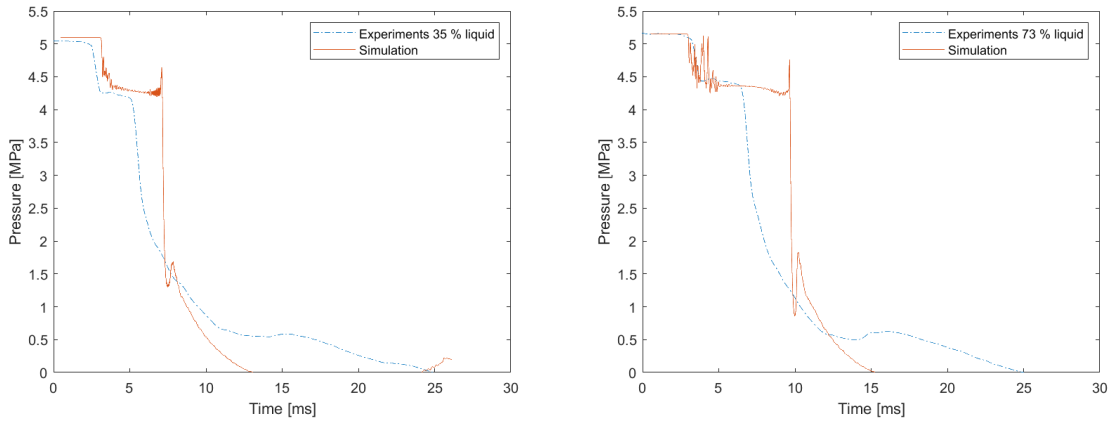

Figure 3: Experimental and simulated pressure history at pressure sensor P2 located 185 mm from the "bottom" of the cone. Left: 35 % liquid volume fraction in the vessel. Right: 73 % liquid volume fraction in the vessel.

Figure 4 (P6) and 5 (P8) shows the experimental and simulated blast waves propagating in the polycarbonate pipe. The activation of the double membrane is done by increasing the pressure in the medium pressure volume up until rupture of the top membrane. The blast wave from this initiation is seen as a pressure peak at about -115 ms in Figure YX (Left) and -15 ms in (Right). The initiation was also included in the simulation, but the time delay is not simulated. The pressure peak from the simulated initiation is seen at about 0 ms for both liquid volume fractions. The reason for including the initiation was to ensure that the polycarbonate pipe had expanded CO2 in it since this will influence the blast wave propagation. The simulated blast from the conical vessel with a liquid volume fraction of 35 % is closer to the experimental results than for 73 %. The blast wave for the 35 % case is dominated by the expansion of the vapor head, while for the 73 % case, the phase transition will significantly impact on the blast wave. Since the simulated pressure drop over the phase transition front in figure 3 is much steeper than the experimental one, it might indicate that the simulated phase transition rate is faster leading to the higher blast pressures seen in the closest pressure transducer (270 mm).

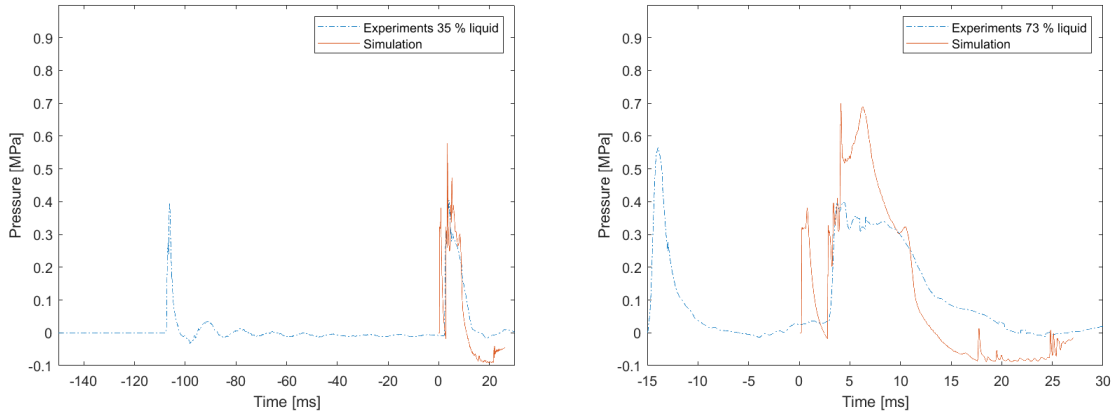

Figure 4: Experimental and simulated pressure history at pressure sensor P6, placed in the polycarbonate pipe at 270 mm above the bottom diaphragm. Left: 35 % liquid volume fraction in the conical vessel. Right: 73 % liquid volume fraction in the conical vessel.

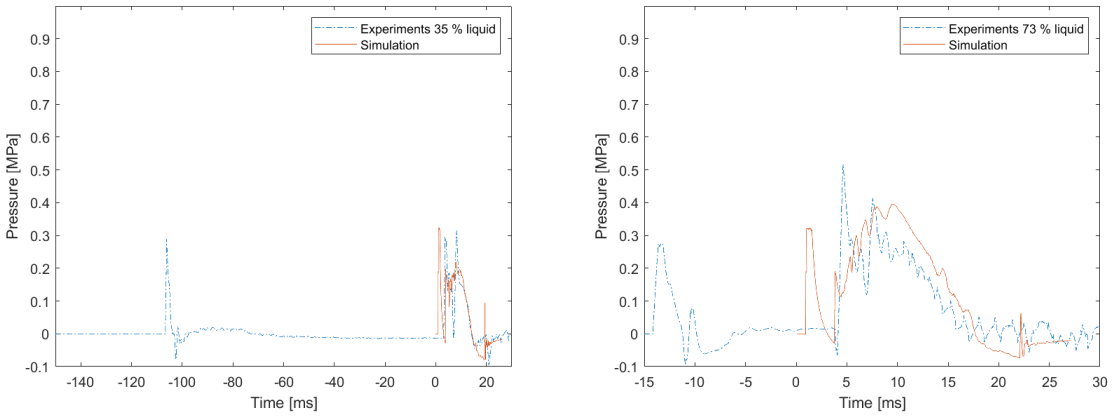

Figure 5: Experimental and simulated pressure history at pressure sensor P8, placed in the polycarbonate pipe at 740 mm above the bottom diaphragm. Left: 35 % liquid volume fraction in the conical vessel. Right: 73 % liquid volume fraction in the conical vessel.

4 Conclusion

The proposed simulation method recreates the main features of the fast depressurization that occurs during a BLEVE scenario. The liquid expansion into a metastable state is captured and the following phase transition rapidly produces gas to generate a blast wave. The simulated blast wave pressure closest to the source is overestimated by the present method due to a too rapid modelled phase transition rate. This overestimation of the phase transition rate is believed to be due to missing dampening effects from earlier onset of nucleation at the wall.

References

[1] Mjaavatten, A. H2 and CO2 thermodynamics. *https://www.github.com/are-mj/thermodynamics*

[2] Span, R. and Wagner, W. A new equation of state for carbon dioxide. *Journal of Physical and Chemical Reference Data*, **25**, 1996, pp. 1509-1596.

[3] Blander, M. and Katz, J. L. Bubble nucleation in liquids. *AlChE Journal*, **21(5),** 1975, pp. 833-848.

[4] Ishii, M. Thermo-fluid dynamic theory of two-phase flow. *Collection de la Direction des Etudes et Recherches d'Electricite de France, No.* **22,** 1975 pp. 275

[5] Ibrahim, O.M., Hansen, P.M., Bjerketvedt, D., Vaagsaether, K. Blast Wave Overpressures from CO_2 Depressurization in a Conical-Shaped Vessel. *10th International Seminar on Fire and Explosion Hazards*, Oslo, Norway, 2022 pp. 86-94. https://hdl.handle.net/11250/3030345